DOI 10.2478/ama-2024-0009

FUZZY BASED SUPERVISION APPROACH IN THE EVENT OF ROTATIONAL SPEED INVERSION IN AN INDUCTION MOTOR

Noura Rezika HATEM BELLAHSENE*

*LTII Laboratory, Department of Automatic, Telecommunications and Electronic, University A. Mira of Bejaia, Bejaia, Algeria

bellahsenehatem@gmail.com

received 12 December 2022, revised 22 July 2023, accepted 23 July 2023

Abstract: This article aims to implement the fuzzy control for an asynchronous motor after a general representation of the vector control. We develop MAMDANI type fuzzy algorithm for MAS speed regulation; it's one purpose is to cancel static error, decrease overshoot, decrease response time, and rise time to obtain an adequate response of the process and regulation and to have a precise, fast, stable and robust system. This paper investigates the design of a fuzzy-based approach for monitoring the inversion of the rotational speed of an induction motor. We will indeed present a robust vector control technique ex-tended to blur in the event of a fault. Direct torque control is known to produce fast and robust response in the AC drive system. However, in a steady state, a rapid and unexpected change in speed can occur which could be dangerous. The performance of the conventional PID controller can be improved by implementing fuzzy logic techniques. The first step is the modelling of the whole system, including the capacitors, the induction generator and the loads. The model is obtained using the Park transformation. The results are thus compared with those of the standard PID control. This approach is applied to a three-phase asynchronous motor (LS90Lz). The presented study improves the transient response time and the precision of the servo system. An inversion of the reference speed of rotation is considered, and the results are very convincing.

Key words: fuzzy control, PID control, Park transformation, speed reversal, vector control, induction motor

1. INTRODUCTION

The use of conventional control techniques re-quires modeling of the process to be controlled. This is not always easy to achieve, especially when it comes to a nonlinear system for which conventional controllers are poorly suited.

To solve this problem, new control strategies, based on the expertise of the operator, have been developed. Among these, the fuzzy control (or regulator) occupies a privileged place. It is characterized by its aptitude to apprehend the problem of nonlinearity.

The fuzzy regulator provides an algorithm that can convert linguistic control strategy based on expert knowledge into an automatic control strategy. Experience has shown that fuzzy logic control gives better results than those obtained by classical control algorithms.

Among many types of machines, three-phase in-duction motors (IMs) benefit from a large popularity. In industry, almost all drive systems use IMs. The adjustable speed IM drives from power electronic converters, which are increasing, phasing out DC drives [1].

The results of conventional supervision methods have been demonstrated in many works for the resolution of practical problems related to the asynchronous motor, such in the industry. Nevertheless, it has been proven that there are still un-answered questions, which can probably be solved by the fuzzy system approach [2–4].

Thus, the advanced supervision methods developed by theorists are only partially able to satisfy the requirements. To overcome these shortcomings, fuzzy modelling can play an important role.

A conventional PID controller is effectively utilized in AC motor electrical drives. The design of conventional PID controllers is more complex when this controller is used in the high rating electrical drives, hence increasing the cost. Soft computing techniques are used in the closed loop control of an electrical system, and it is known as advanced intelligent control.

Nowadays, the intelligent control is playing an essential role in industries control. Intelligent control techniques can be implemented using microprocessors and microcontrollers which have high computation ability, and which operate at high speed [5, 6].

The asynchronous motor is modelled by Park's equations to facilitate calculations and simplify representations [7-12]. The modelling of the asynchronous motor requires certain simplifying assumptions to obtain simple relations.

It will thus be assumed that the self-inductances are constant [12–19], the mutual inductances are considered according to the position of their magnetic axes and the rotor resistances are constant with respect to the rotational speed axes and the rotor resistances are constant with respect to the rotational velocity [20–25].

2. THREE PHASES AM MODELING

The rotor can be modelled by three identical windings staggered in space by 120°. These windings are short-circuited, and the voltage across them is zero. We pose "θ" the electrical angle between the phase 'A' stator and the phase 'a' rotor as shown in Fig. 1.

DOI 10.2478/ama-2024-0009

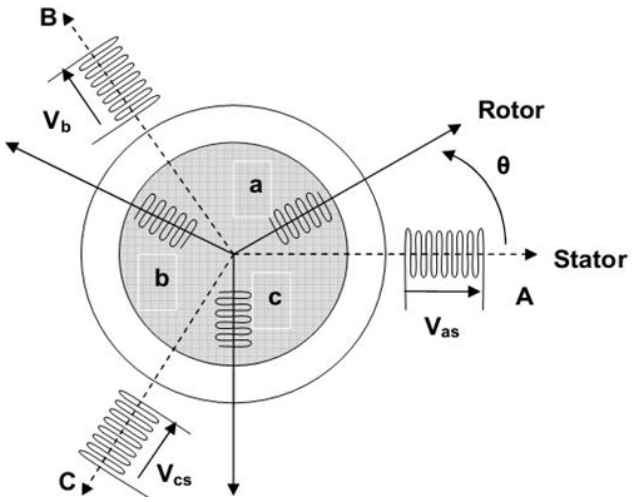

Fig. 1. Schematic representation of three-phases AM

The modelling of the asynchronous machine requires certain simplifying assumptions in order to obtain simple relations; this it will be assumed that the self-inductances are constant, the mutual inductances are a function of the position of their magnetic axes and the rotor resistances are constant with respect to the speed of rotation.

– Electrical equations

By applying Ohm's law and Faraday's law to the windings of the stator and the rotor, we find a writing in the matrix form:

$$[V_s] = [R_s][I_s] + \frac{d}{dt}[\Phi_s]$$
$$[V_r] = [0] = [R_r][I_r] + \frac{d}{dt}[\Phi_r]$$

– Magnetic equations (of flows)

The totalized fluxes coupled between the stator and rotor phases are expressed in the form:

$$[\Phi_s] = [L_{ss}][I_s] + [M_{sr}][I_r]$$

$$[\Phi_r] = [L_{rr}][I_r] + [M_{sr}]^t[I_s]$$

By replacing the magnetic equations in electrical equations, we obtain the two expressions of the stator and rotor voltages:

$$[V_s] = [R_s][I_s] + [L_{ss}]\frac{d}{dt}[I_s] + \frac{d}{dt}\{[M_{sr}][I_r]\}$$

$$[V_r] = [R_r][I_r] + [L_{rr}]\frac{d}{dt}[I_r] + \frac{d}{dt}\{[M_{sr}]^t\,[I_s]\}$$

– Mechanical equations

The torque $C_e\frac{1}{2}$

Movement (speed) $J\frac{d\Omega}{dt} + F\Omega = C_e - C_r$

m_s, m_r: Mutual inductances between phases, stator and rotor.

l_s, l_r: Proper, stator and rotor inductances of a phase.

L_{ss}, L_{rr}: Stator and rotor induction matrix.

M_{sr}, M_{sr}: Matrix of mutual inductances stator_rotor and rotor_stator.

θ: Angle between the rotor axis and the stator axis.

$C_r = F.\Omega$: Resistant torque.

$\Omega = \frac{\omega_r}{p}$: mechanical angular speed of the rotor.

J: moment of inertia.

F: Coefficient of friction.

3. PARK MODEL

The machine equations can be further simplified by choosing a particular frame of reference for dq. The choice of benchmark is made according to the purpose of the application. Three types of benchmarks can be considered, namely:

– Referencial linked to the stator (α,β) : It is interesting during the study of significant variation of the speed of rotation seen that appears in the equation.

– Referencial linked to the rotor (x,y): It is interesting when studying transient regimes where the speed is considered constant.

– Referencial linked to in the rotating field (d,q): It eliminates the influence of rotor and stator leakage reactances.

The referencial linked to in the rotating field (d,q) is the repository which is chosen during our study (Fig .2), because it has advantages when studying the loads around a given point. The advantage of using this model is to have constant quantities in steady state. It is then easier to regulate it.

The temporal simulation of instantaneous electrical and mechanical quantities, considering the diffusive character of the skin effect in the rotor, requires adapting the model of Park in order to isolate the non-integer order transfer function representing the rotor. To simplify the representation of the previous equations, we introduce the transformation of Park, obtained using the matrix P, which consists in moving from a three-phase winding to a biphase winding and vice versa [3].

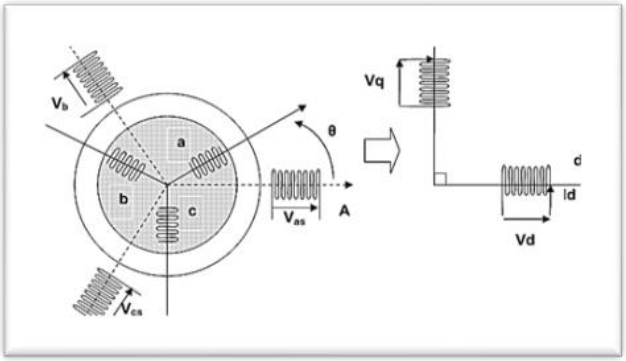

Fig. 2. Asynchronous machine Park model

The change of variables relating to currents, voltages and fluxes is given by the transformation:

$$\begin{bmatrix} X_d \\ X_q \\ X_0 \end{bmatrix} = P(\theta)\begin{bmatrix} X_a \\ X_b \\ X_c \end{bmatrix}, \begin{bmatrix} X_a \\ X_b \\ X_c \end{bmatrix} = P(\theta)^{-1}\begin{bmatrix} X_d \\ X_q \\ X_0 \end{bmatrix}$$

With [X] is tension, courant or flux and the matrixes $P(\theta)$ and $P(\theta)^{-1}$ are given as follows:

$$P(\theta) = \sqrt{\frac{2}{3}}\begin{bmatrix} cos(\theta) & cos\left(\theta - \frac{2\pi}{3}\right) & cos\left(\theta + \frac{2\pi}{3}\right) \\ -sin(\theta) & -sin\left(\theta - \frac{2\pi}{3}\right) & -sin\left(\theta + \frac{2\pi}{3}\right) \\ \sqrt{\frac{1}{2}} & \sqrt{\frac{1}{2}} & \sqrt{\frac{1}{2}} \end{bmatrix}$$

DOI 10.2478/ama-2024-0009

$$P(\theta)^{-1} = \sqrt{\frac{2}{3}} \begin{bmatrix} cos(\theta) & -sin(\theta) & \sqrt{\frac{1}{2}} \\ cos\left(\theta - \frac{2\pi}{3}\right) & -sin\left(\theta - \frac{2\pi}{3}\right) & \sqrt{\frac{1}{2}} \\ cos\left(\theta + \frac{2\pi}{3}\right) & -sin\left(\theta + \frac{2\pi}{3}\right) & \sqrt{\frac{1}{2}} \end{bmatrix}$$

Where θ is the electrical angle between the stator phase 'A' and the rotor phase 'a'.

The application of the Park transform gives rise to the equations:

$$\begin{bmatrix} V_{ds} \\ V_{qs} \end{bmatrix} = \begin{bmatrix} R_s & 0 \\ 0 & R_s \end{bmatrix} \begin{bmatrix} I_{ds} \\ I_{qs} \end{bmatrix} + \frac{d}{dt} \begin{bmatrix} \Phi_{ds} \\ \Phi_{qs} \end{bmatrix} + \begin{bmatrix} 0 & -w_s \\ w_s & 0 \end{bmatrix} \begin{bmatrix} \Phi_{ds} \\ \Phi_{qs} \end{bmatrix}$$

$$\begin{bmatrix} V_{dr} \\ V_{qr} \end{bmatrix} = \begin{bmatrix} R_r & 0 \\ 0 & R_r \end{bmatrix} \begin{bmatrix} I_{dr} \\ I_{qr} \end{bmatrix} + \frac{d}{dt} \begin{bmatrix} \Phi_{dr} \\ \Phi_{qr} \end{bmatrix} + \begin{bmatrix} 0 & -w_r \\ w_r & 0 \end{bmatrix} \begin{bmatrix} \Phi_{dr} \\ \Phi_{qr} \end{bmatrix}$$

$$\begin{bmatrix} \Phi_{ds} \\ \Phi_{qs} \end{bmatrix} = \begin{bmatrix} L_s & 0 \\ 0 & L_s \end{bmatrix} \begin{bmatrix} I_{ds} \\ I_{qs} \end{bmatrix} + \begin{bmatrix} M & 0 \\ 0 & M \end{bmatrix} \begin{bmatrix} I_{dr} \\ I_{qr} \end{bmatrix}$$

$$\begin{bmatrix} \Phi_{dr} \\ \Phi_{qr} \end{bmatrix} = \begin{bmatrix} L_r & 0 \\ 0 & L_r \end{bmatrix} \begin{bmatrix} I_{dr} \\ I_{qr} \end{bmatrix} + \begin{bmatrix} M & 0 \\ 0 & M \end{bmatrix} \begin{bmatrix} I_{ds} \\ I_{qs} \end{bmatrix}$$

After calculations, writing in the matrix form, the electric and magnetic equations are given as follows:

$$\begin{bmatrix} V_{ds} \\ V_{qs} \\ 0 \\ 0 \end{bmatrix} = \begin{bmatrix} (R_s + L_s S) & -L_s\omega_s & MS & -M\omega_s \\ L_s\omega_s & (R_s + L_s S) & M\omega_s & MS \\ MS & -\omega_{gl}M & (R_s + L_s S) & -\omega_{gl}L_r \\ \omega_{gl}M & MS & \omega_{gl}L_r & (R_r + L_r S) \end{bmatrix} \begin{bmatrix} I_{ds} \\ I_{qs} \\ I_{dr} \\ I_{qr} \end{bmatrix}$$

The courant equations are given:

$$I_{ds} = \frac{L_r}{L_s L_r - M^2}\Phi_{ds} - \frac{M}{L_s L_r - M^2}\Phi_{dr}$$

$$I_{qs} = \frac{L_r}{L_s L_r - M^2}\Phi_{qs} - \frac{M}{L_s L_r - M^2}\Phi_{qr}$$

$$I_{dr} = \frac{L_s}{L_s L_r - M^2}\Phi_{dr} - \frac{M}{L_s L_r - M^2}\Phi_{ds}$$

$$I_{qr} = \frac{L_s}{L_s L_r - M^2}\Phi_{qr} - \frac{M}{L_s L_r - M^2}\Phi_{qs}$$

The determination of the instantaneous electromagnetic torque in a machine can be carried out in two ways: by an instantaneous power balance or by the so-called "virtual work" method.

We will use the first method. The instantaneous electrical power supplied to the stator and rotor windings as a function of the axis sizes d,q is given by the following expression:

$$P_e = V_{ds}I_{ds} + V_{qs}I_{qs} + V_{dr}I_{dr} + V_{qr}I_{qr}$$

However, the electromechanical power is related to the electromagnetic torque by the following expression:

$$C_e = \frac{P_{em}}{\Omega} = p.\frac{P_{em}}{\omega}$$

However, the electromechanical power is related to the electromagnetic torque by the following expression:

$$C_e = p\frac{M}{L_r}\left(\Phi_{dr}I_{qs} - \Phi_{qr}I_{ds}\right)$$

It can be seen that the electromagnetic torque equation is not linear, due to the cross product of the current and flux components (coupling).

4. AM VECTOR CONTROL

The principle of vector control (Fig. 3) is to have an operation similar to that of a DC motor with independent excitation, where there is a natural decoupling process between the quantity controlling the flux (the excitation current) and that linked to the torque (the armature current). This decoupling makes it possible to obtain a very fast torque response.

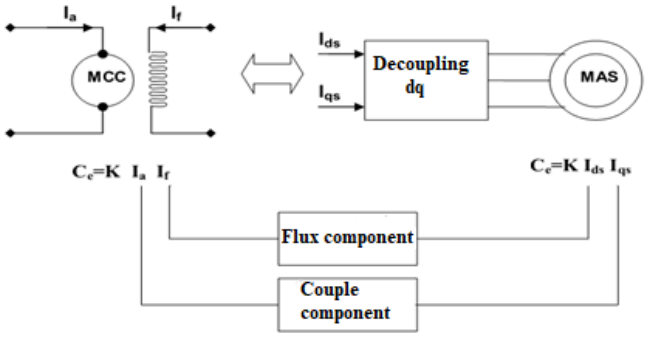

Fig. 3. Diagram of the decoupling principle for AM by analogy with MCC

Several strategies are possible such as:

1. Orientation of the stator flux: $\Phi_{ds} = \Phi_s$ and $\Phi_{qs} = 0$
2. Orientation of the rotor: $\Phi_{dr} = \Phi_r$ and $\Phi_{qr} = 0$
3. Orientation of the air gap: $\Phi_{de} = \Phi_e$ and $\Phi_{qe} = 0$

We will limit ourselves to exposing the command with oriented rotor flux ($\Phi_{dr} = \Phi_r$ and $\Phi_{qr} = 0$) (Fig. 4), whose principle is to cancel the flux Φ_qr ; it is based on:

– Maintaining the flux Φ_dr constant and aligned on the axis d of the reference d - q by action on current I_ds.
– Electromagnetic torque control by action on the current I_qs.

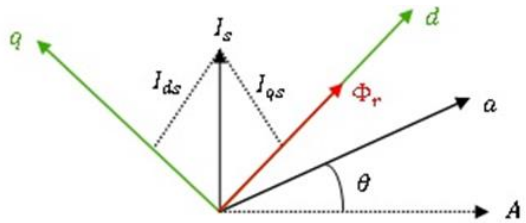

Fig. 4. Command with oriented rotor flux

The torque is given then by $C_e = P\frac{M}{L_r}\left(\Phi_{dr}I_{qs}\right)$

The equations of tensions on the reference (d,q) are given as follows:

$$V_{ds} = R_s I_{ds} + L_s\frac{dI_{ds}}{dt} - \omega_s L_s I_{qs} + M\frac{dI_{dr}}{dt} - \omega_s M I_{qr}$$

$$V_{qs} = R_s I_{qs} + L_s\frac{dI_{qs}}{dt} - \omega_s L_s I_{ds} + M\frac{dI_{qr}}{dt} + \omega_s M I_{dr}$$

$$0 = M\frac{dI_{ds}}{dt} - (\omega_s - \omega_m)MI_{qs} + L_r\frac{dI_{dr}}{dt} + R_r I_{dr} - (\omega_s - \omega_m)L_r I_{qr}$$

$$0 = M\frac{dI_{qs}}{dt} - (\omega_s - \omega_m)MI_{ds} + L_r\frac{dI_{qr}}{dt} + R_r I_{qr} + (\omega_s - \omega_m)L_r I_{dr}$$

$$With\ \omega_s = \omega_m + \frac{MR_r}{L_r\Phi_{rd}}I_{qs}$$

The rotor current equations are given:

DOI 10.2478/ama-2024-0009

$$V_{ds} = R_s I_{ds} + \sigma L_s \frac{dI_{ds}}{dt} + \frac{M}{L_r}\frac{\Phi_{dr}}{dt} - \omega_s \sigma L_s I_{qs}$$

$$V_{qs} = R_s I_{qs} + \sigma L_s \frac{dI_{qs}}{dt} + \omega_s \frac{M}{L_r}\Phi_{dr} + \omega_s \sigma L_s I_{ds}$$

$$MI_{ds} = \Phi_{dr} + \frac{L_r}{R_r}\frac{d\Phi_{dr}}{dt}$$

The classical PID diagram is given in Fig.5.

The PID parameters, according to Fig.5, are given as follows

$$K_d = P.\frac{M}{L_r}.\Omega_r, K_p = \frac{2.\varepsilon.\omega_n.J+F}{Ke}, K_i = \frac{\omega_n^2.J}{Kp.Ke}$$

K_p=9.25, K_d=0 *and* K_i=6.25) ($\omega_n = 16rd$: proper pulsation, $\varepsilon = 0.7$: damping factor).

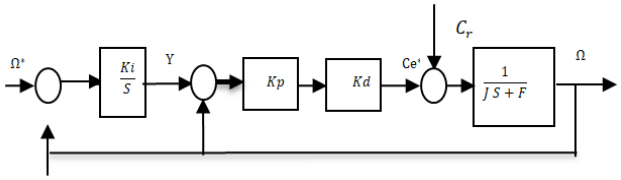

Fig. 5. PID control topology

5. FUZZY LOGIC CONTROL DESIGN

The fuzzy logic regulator (FLR) takes its place in the control chain as shown in (Fig. 6).

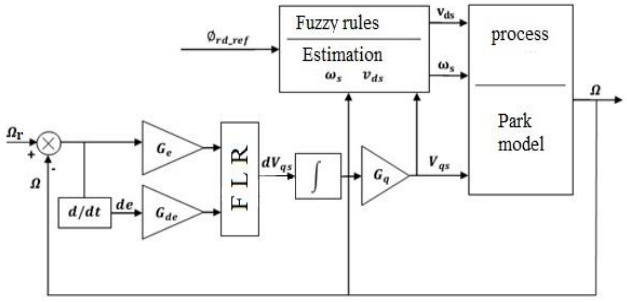

Fig. 6. Fuzzy-logic control design

Input variables are mostly error '*e*' and the change-of-error '*de*' regardless of complexity of controlled plants. Alternatively, the change of control input is used as its output variable. The parameters of the motor are calculated: the rotor time constant (Tr=0.0720 s) and the Blondel dispersion coefficient ($\sigma = 0.1134$). Fig. 7 provides the fuzzy regulator chain.

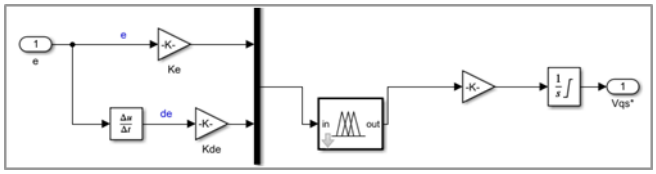

Fig. 7. The fuzzy regulator

A table of fuzzy rules (Table I) is then constructed on a two-dimensional (2-D) space. The output is calibrated to allow it to vary in the domain accepted by the system. For reasons of simplification during the simulation, we adopt as membership functions, those having the triangular form distributed in a uniform and equidistant manner with symmetrical forms. The interval of interest for each input variable, namely the error e and the variation in the error, is subdivided into three classes (subsets). Regarding the variation of the order, it is subdivided into seven classes as well. Each of these classes is associated with a membership function.

The distribution of membership functions in their respective universes of discourse is given in Fig. 8, Fig. 9, and Fig. 10. The adjustment strategy mainly depends on the inferences adopted. The fuzzy input-based inference engine uses the "If…Then" property of rules in the knowledge base to make decisions.

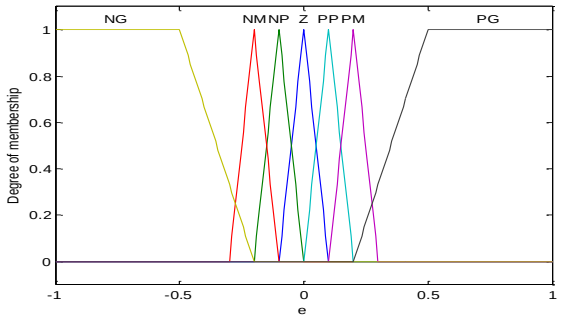

Fig. 8. Input 'e' membership functions

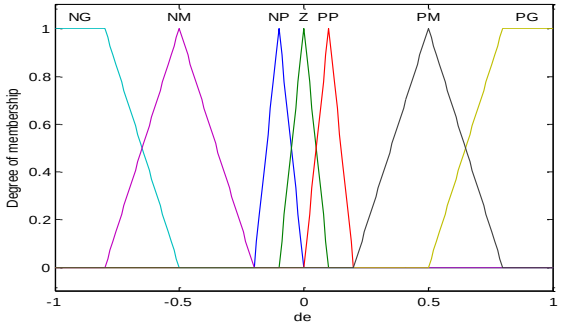

Fig. 9. Input 'de' membership functions

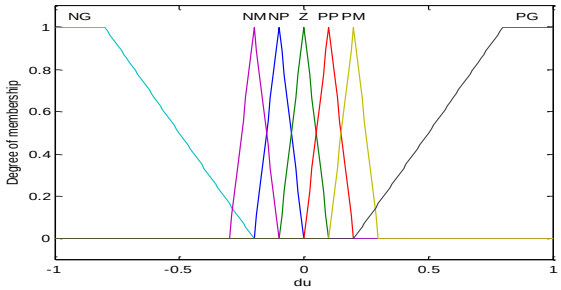

Fig. 10. Output 'du' membership functions

Tab .1. Table of fuzzy control rules

e \ de	NG	NM	NP	Z	PP	PM	PG
NG	NG	NG	NG	NG	NG	NG	Z
NM	NG	NG	NM	NP	NP	Z	PG
NP	NM	NM	NP	NP	Z	PP	PP
Z	NG	NG	NP	Z	PP	PG	PG
PP	NP	NP	Z	PP	PP	PM	PM
PM	NP	Z	PP	PP	PM	PM	PG
PG	Z	PP	PP	PM	PM	PG	PG

DOI 10.2478/ama-2024-0009

In our case, the inferences specify how the linguistic value of the variable of the command du is calculated according to the linguistic values of e and de. Given the advantages it offers, MAMDANI's Max-Min inference method is chosen in our application. The decision rules consist of situation/action pairs of the form:

If *e* is *A* AND *de* is *B*, then *du* is *C*.

This set of rules should regroup all the possible situations of the system evaluated for the different values assigned to *e* and of and all the corresponding values of *du*.
The decision table that we have chosen in our work is the famous MAC VICAR-WHELAN rule base (Table I) with inputs (*e*: error, *de*: derivative of error) and the output (*du*).

This rule base is organized in the form of a symmetrical diagonal inference table; it can be deduced for example according to a temporal analysis which consists in comparing the response of the system to the instruction according to the objectives fixed in closed loop.

($e = \Omega_r - \Omega$) with (Ω_r : reference speed) is the derivative of the error and sometimes of the integral of the error. The output "*du*" of the regulator can be the torque variation (dCe), either the variation of the current (dIqs) or the variation of the voltage (dVqs).

(FLR parameters are Gq=3000; Ke=1/12 and Kde=1/600). Defuzzification is the last stage of the regulator; it converts the linguistic value of du (variation of the action) into a numerical value. Our choice fell on the method of defuzzification of the center of gravity for its simplicity and its performance.

6. APPLICATION

The characteristics of the asynchronous machine are shown in Tab. 2- 5.

Tab. 2. Mechanical parameters

Nominal power	$P_n = 1500$	W
Synchronism speed	$N = 1420$	$tr\ /\ min$
Rated load torque	$C_r = 10$	$N.m$
Tension	$V = 220/380$	V
Nominal current	$I = 6.31/3.64$	A
Synchronism frequency	$f_s = 50$	Hz
Yield	$\eta = 0.78$	%
Flux	$\Phi = 0.7$	Wb

Tab. 3. Controller setttings

$K_e = 1\ /\ 150$	$Kp\ =\ 9.25$
$K_{de} = 1\ /\ 1500$	$Ki\ =\ 6.25$
$G_q = 300000$	

Tab. 4. Machine electrical characteristics

Stator resistance	$R_s = 4.85$	Ω
Rotor resistance	$R_r = 3.805$	Ω
Stator duty cycle inductance	$L_s = 0.274$	H
Rotor cyclic inductance	$L_r = 0.274$	H
Mutual cyclic inductance	$M = 0.258$	H
Rotor time constant.	$T_r = L_r\ /\ R_r$	
Blondel dispersion coefficient	$\sigma =\ 1 - (M^2\ /\ L_s\ L_r)$	

Tab. 5. Nominal parameters

Moment of inertia	$J = 0.031$	$Kg.m^2$
Friction coefficient	$F = 0.0081$	$N.m.s\ /\ rad$

7. RESULTS AND DISCUSSION

Vector control has been applied to the asynchronous machine. The figures Fig.11, Fig.12, Fig,13 and Fig.14 give graphs of the response of each parameter (Fluxdr, Fluxqr, stator current component Iqs and stator current) of the motor at no load.

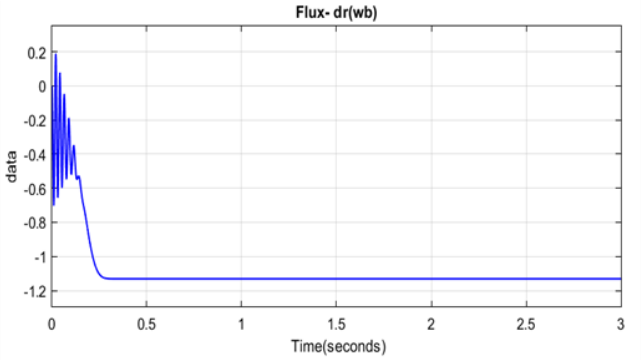

Fig. 11. Flux-dr response at no load

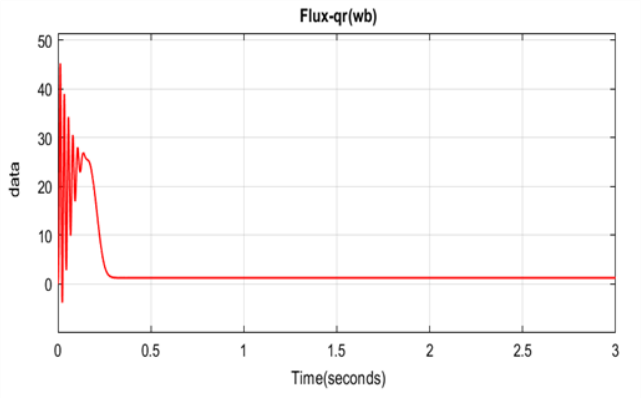

Fig. 12. Flux-qr response at no load

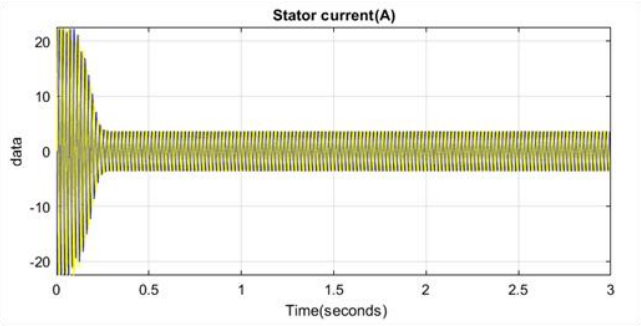

Fig. 13. Stator current response at no load

The responses of the IM model, for a reference speed of 150 rad/s, are given below.

The curves in figures (Fig. 15-19) detail separately the evolution of the characteristics of the MAS in load of 10 N.m applied

DOI 10.2478/ama-2024-0009

from 0.75 for 1s. The results show that when the motor is acted upon by resistive torque $Cr = 10N{\cdot}m$, the velocity exceeds the reference value and then decreases to 148 rad/s (Fig. 15).

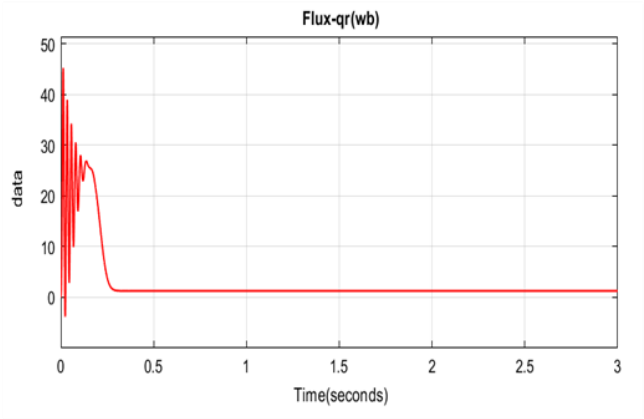

Fig. 14. Stator current component Iqs response at no load

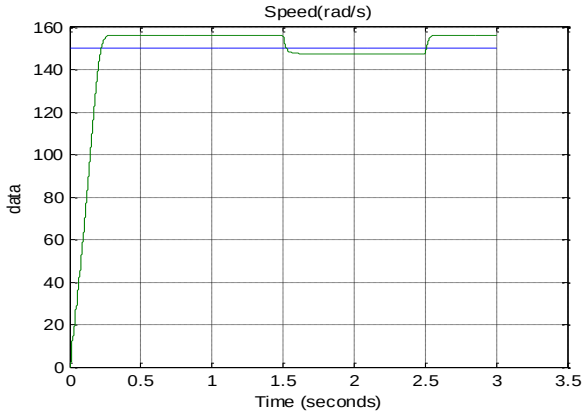

Fig. 15. Velocity response

The stator current increases to its nominal value and the stator current (Fig. 16) following axis Iqs decreases and stabilizes at −5.2 A.

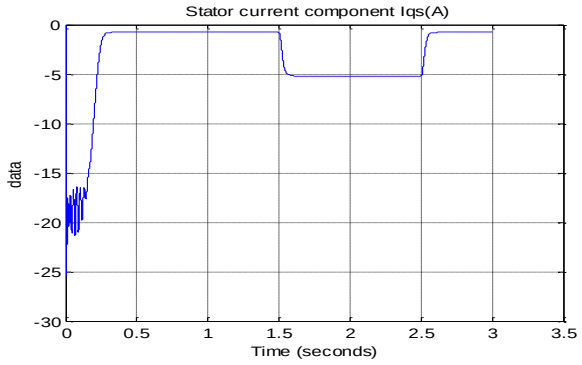

Fig. 16. Stator current component Iqs response

The torque (Fig. 17) also increases until it reaches the value to drive the load and the rotor fluxes (Fig. 18) and (Fig. 19) increase and stabilize, respectively, at −0.15 Wb and 0.1 Wb.

Regarding to the PID controller and taking in account the AM characteristics, the parameters considered are Kp=9.25, Kd=0 and Ki=6.25. The fuzzy responses of the regulator are compared with those given by the PID regulator. The results are shown in the figures below.

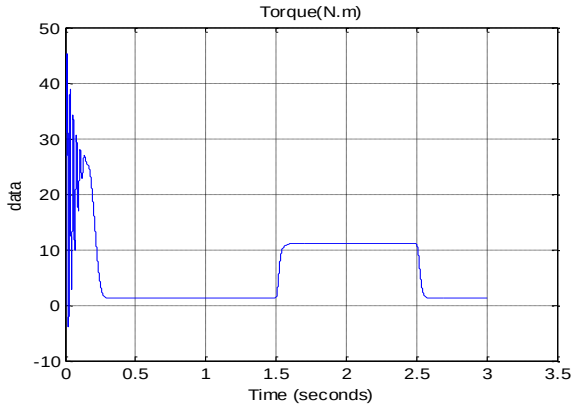

.

Fig.17. Torque response

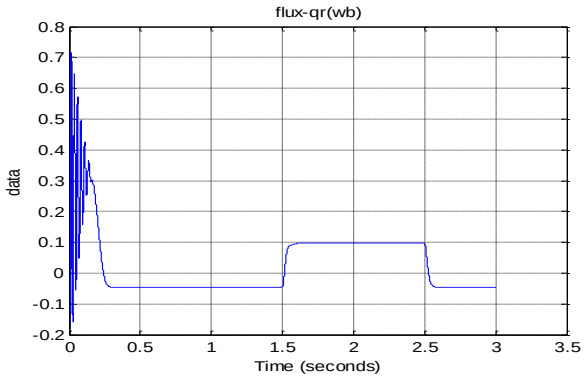

Fig. 18. Flux-qr response

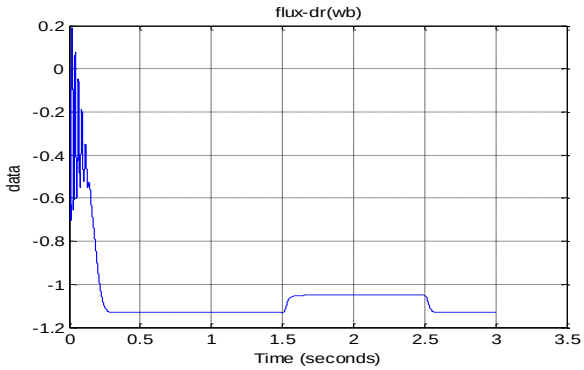

Fig. 19. Flux-dr response

The torque oscillation (Fig. 20) reaches the maximum value of the order of 4.5 times the nominal torque (rises to more than 45.27 N·m).

This is due to noises generated by mechanical parts. After the disappearance of the transient regime which lasts 0.16s, the torque decreases almost linearly from 26.9 N · m and tends towards zero.

The minimum value is 0.314 N · m; it is due to friction. These results show that the two types of control demonstrate good performance for Fluxq_r (Fig. 21) and Flux_dr (Fig. 22) and stator current component Iqs (Fig. 22).

DOI 10.2478/ama-2024-0009

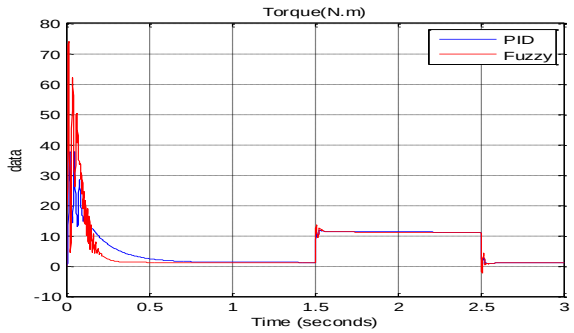

Fig. 20. Torque response

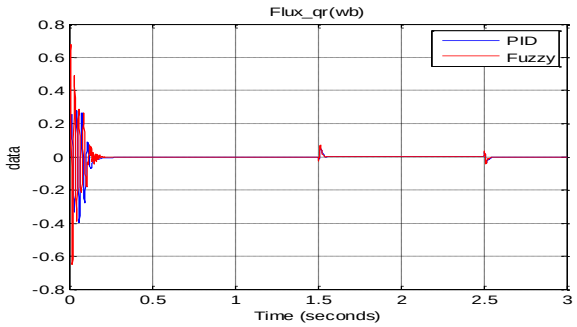

Fig. 21. Flux_qr response

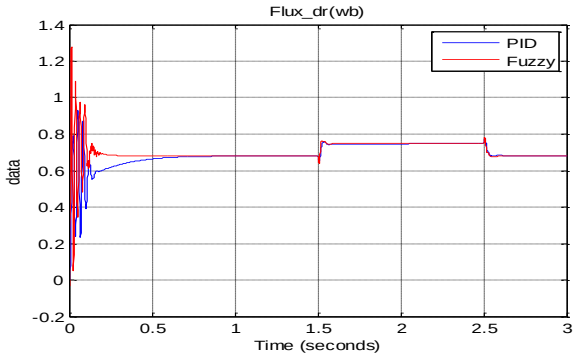

Fig. 22. Flux_dr response

We find almost the same situation with the only difference in response time of speed; the response time of the PI controller is always the same under all conditions, but that of the fuzzy controller depends on the set point.

In transient mode, mains supply shows a high current demand of 27.06 A (Fig. 23). After its disappearance, the steady state is reached.

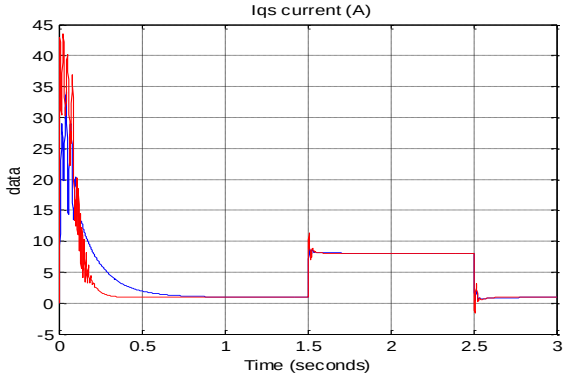

Fig. 23. Stator current component Iqs response

During start-up and in the transient state, the rotational speed increases and evolves with a rise time of 0.2 s, at t = 0.3 s (start of the steady state); it stabilizes at a value close to the set point velocity (156.7 rad/s) (Fig. 24).

We observe a perfect continuation of the reference velocity, an insensitivity and rapid rejection of the load (0.88%).

Let us now consider the case where the motor is in the final position and an unknown load at some frequency is applied to the motor shaft.

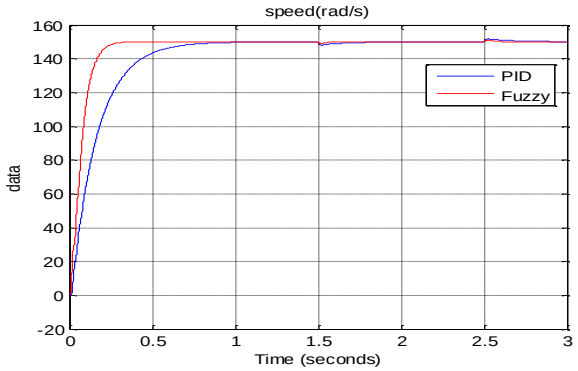

Fig. 24. Velocity response

An inversion of the reference rotational speed (Fig. 25) occurs after 1 s and a load of 10 N·m at 2 s from the start.

The output (Fig. 26) has a good follow-up of the set point; the current Iqs does not have an overshoot during this inversion.

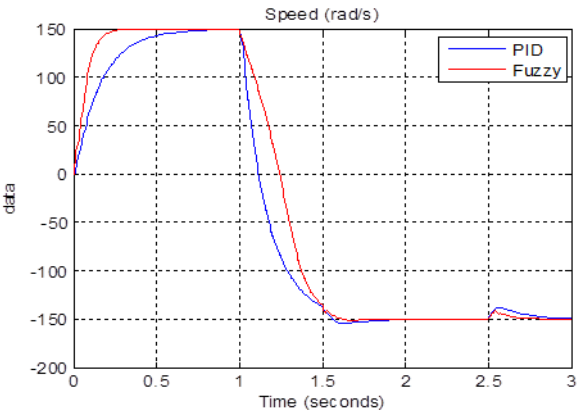

Fig. 25. Rotational speed response

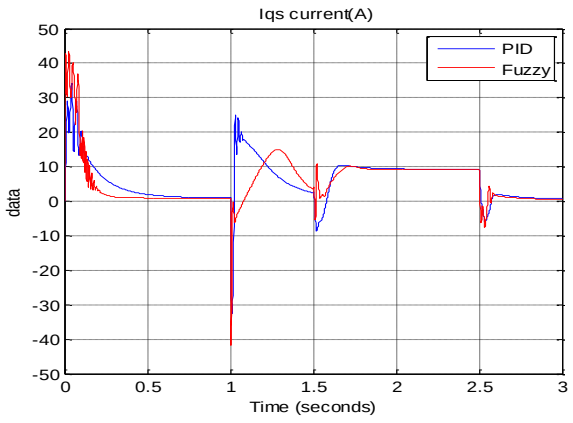

Fig. 26. Iqs current response

This difference is due to the fact that the response time of the PI regulator is determined by its design ; it always manages on its first rise to catch up with 95% of its reference value within the regulation time ; if this time is fast compared with the machine, we notice an overshoot.

The fuzzy controller, on the other hand, finds a different response time each time because this time is not determined in its design, and overshoot is always acceptable.

Therefore, these results show that the two types of control give good performance ; we find almost the same with the only difference in terms of the speed response time; the response time of the PI regulator is always the same under all conditions ; on the other hand, that of the fuzzy regulator depends on the set point value ; the closer this value is to the initial value, the faster the response.

The control strategy with the fuzzy logic has been applied to the AM, and the results of simulation have proved the efficiency of control of the system whose required performance indicators were fully met, namely:

- An appreciable rise time.
- A negligible excess.
- A good pursuit of the set-point.
- Rejection of the disturbance.
- The speed of reversal of the direction of rotation.

The fuzzy control greatly improves the behavior and the efficiency of the vector control and thus allows obtaining a high-performance variable speed drive which is justified by the results obtained by comparing the vector control with conventional PI regulators and by fuzzy logic controllers. The fuzzy controller improves the robustness of the vector control; the simulations show that the errors converge towards negligible static values which give good control results.

The results of this approach based on field-oriented control and fuzzy logic regulator are very conclusive as long as they do not differ too much from the results already seen with the same regulator in the event that the engine parameters do not vary. However, we see a slightly higher response time.

8. CONCLUSION

The PID control often displays low performance. Overshoot and rise times are tightly coupled, making gain adjustments difficult. In this article, we have presented the results obtained by applying the fuzzy control, which considerably improves the behavior and the efficiency of the vector control.

Fuzzy logic extended vector control provides a diagnostic approach to significantly decouple overshoot and rise time, allowing for easy setup and very high load rejection characteristics.

The presented study improves the transient response time and the precision of the servo system. An inversion of the reference rotational speed is considered, and the results are very consistent.

Considering these results, we find a perfect tracking reference speed, insensitivity, and rapid rejection of loads, as well as a decoupling of the d-q axes which is not influenced by the regime applied to the machine.

The fuzzy control improves the behavior and efficiency of the vector control and thus makes it possible to obtain a variable speed drive that is more stable and robust to faults.

Analysis of variations in machine parameters such as electromagnetic torque, stator and rotor currents in the Park's mark is used to detect the presence of defects.

The control developed adapts to the sudden change in behavior such as a speed reversal.

Time will show whether these theoretical concepts represent a sufficient degree of improvement over the existing techniques to enter the domain of commercial drives.

However, and through this study, it appears that the major shortcoming of fuzzy logic control is that it depends on human expertise. The rules of a fuzzy logic control system must be regularly updated.

As, perspectives, the artificial neuronal networks (ANNs) can be combined with fuzzy logic to improve the control, extending the IM driver life, and achieving proper motor operation and performance is significant. In this case, artificial intelligence (AI) is a helpful tool to match the motor parameter values and the data needed by the controller.

REFERENCES

1. Trzynadlowski AM. Control of Induction Motors. Academic Press. 2001; ISBN 9780127015101; Nevada. https://doi.org/10.1016/B978-012701510-1/50000-3
2. PREMKUMAR K, THAMIZHSELVAN T, PRIY M, Vishnu et al. Fuzzy anti-windup pid controlled induction motor. International Journal of Engineering and Advanced Technology. 2019; 9(1): 184-189.
3. Korbut M, Szpica D. A Review of Compressed Air Engine in the Vehicle Propulsion System. Acta Mechanica et Automatica. 2021;15(4): 215-226. https://doi.org/10.2478/ama-2021-0028
4. https://www.researchgate.net/profile/Drkmkumar/publication/337285022_Fuzzy_Anti-indup_PID_Controlled_Induction_Motor/
5. Mehidi IM, SAAD N, MAGZOUB M and al. Simulation analysis and experimental evaluation of improved field-oriented controlled induction motors incorporating intelligent controllers. IEEE Access. 2022;10: 18380-18394 Design and Simulation of Neuro-Fuzzy Controller for Indirect Vector-Controlled Induction Motor Drive SpringerLink.
6. Roose A, Yahya S, and Al-Rizzo H Fuzzy-logic control of an inverted pendulum on a cart. Computers & Electrical Engineering, Elsevier. 2017.
7. Badr B, Eltamaly A M, and Alolah. Fuzzy controller for three phases induction motor drives. IEEE Vehicle Power and Propulsion Conference, Sept. 2010. https://doi.org/10.1109/VPPC.2010.5729080
8. Achbi M, Kehida S, Mhamd Lan and Hedi D A Neural-Fuzzy Approach for Fault Diagnosis of Hybrid Dynamical Systems: Demonstration on Three-Tank System" Acta Mechanica et Automatica. 2021; 15 (1): 1-8. https://doi.org/10.2478/ama-2021-0001
9. Khan F, Sulaimanandand and Ahmad Z Review of Switched Flux Wound-Field Machines Technology. IETE Technical Review, 2016.
10. Zerdali E, Met A, Barkak A and Erkan M Computationally efficient predictive torque control strategies without weighting factors Turkish Journal of Electrical Engineering and Computer Sciences.2022; 30 (6). https://doi.org/10.55730/1300-0632.3955
11. Ananthamoorthy N and Baskaran K. Velocity and torque control of permanent magnet synchronous motor using hybrid fuzzy proportional plus integral controlle. Journal of Vibration and Control, SAGE Publications. 2013; 20–29.
12. Aissaoui A, Abid M. A fuzzy logic controller for synchronous machine. Journal of Electrical Engineering. 2007; 285–290.
13. Bharathi Y and. al., “Multi-input fuzzy logic controller for brushless DC motor drives”, Defence Science Journal. 2008; 58 (1): 147–158. https://doi.org/10.14429/dsj.58.1632
14. Faiz J, Manoochehri M, Shahgholia G. Performance improvement of a linear permanent magnet synchronous drive using fuzzy logic controller. Proceedings of IEEE International Conference on Power System Technology, Oct. 2010. https://doi.org/10.1109/POWERCON.2010.5666041

15. Soundarajan A, Sumathi A. Fuzzy based intelligent controller for power generating stations. Journal of Vibration and Control. 2011 (17): 214–227. https://doi.org/10.1177/1077546310371347
16. Ozturk N. Celik Educational Tool for the Genetic Algorithm-Based Fuzzy Logic Controller of a Permanent Magnet Synchronous Motor Drive. International Journal of Electrical Engineering Education. SAGE Publications. 2014. https://doi.org/10.7227/IJEEE.51.3.4
17. Bharathi Y and al. Multi-input fuzzy logic controller for brushless DC motor drives. Defence Science Journal. 2008; 58 (1): 147–158. https://doi.org/10.14429/dsj.58.1632
18. Ruiz J, Espinosa A, Romeral L. An introduction to fault diagnosis of permanent magnet synchronous machines in master's degree courses. Comput. Appl. Eng. Educ. 2010; published online.
19. Siavashi E, Pahlavanhoseini R, Pejmanfar A. Using Clonal Selection Algorithm to optimize the Induction Motor Performance. Canadian Journal on Electrical and Electronics Engineering. 2011; 2 (9).
20. Zidani F, Nait Said R. Direct Torque Control of Induction Motor with Fuzzy Minimization Torque Ripple. Journal of Electrical Engineering. 2005; 56 (7–8): 183–188.
21. Ameur F. Application of Fuzzy Logic for a Ripple Reduction Strategy in DTC Scheme of a PWM Inverter fed Induction Motor Drives. Journal of Electrical Systems. 2009; 1: 13–17.
22. Gadoue S, Giaouris D and Finch J. Artificial intelligence-based speed control of DTC induction motor drives: A comparative study. Electric Power Systems Research.2009; 79 (1): 210–219. https://doi.org/10.1016/j.epsr.2008.05.024
23. Liu S, Wang M, Chen Yand Li. SA Novel Fuzzy Direct Torque Control System for Three-level Inverter-fed Induction Machine .International Journal of Automation and Computing. 2020; 7 (1): 78–85. https://doi.org/10.1007/s11633-010-0078-7
24. Pasamontes M and al. Learning switching control: A tank level-control exercise," IEEE Trans. Educ. 2012; 55 (2): 226–232. https://doi.org/10.1109/TE.2011.2162239
25. Guven U, Sonmez Yand Birogul SA. Computer based educational tool for fuzzy logic-controlled DC-DC converters. J. Polyt. 2007; 10: 339–346.

Noura Rezika H. Bellahsene: https://orcid.org/0000-0002-6644-9930